Taylor & Francis
Taylor & Francis Group

Exploration Geophysics

ISSN: 0812-3985 (Print) 1834-7533 (Online) Journal homepage: https://www.tandfonline.com/loi/texg20

Geological significance of delineating paleochannels with AEM

Subash Chandra, Joy Choudhury, Pradip K. Maurya, Shakeel Ahmed, Esben Auken & Saurabh K. Verma

To cite this article: Subash Chandra, Joy Choudhury, Pradip K. Maurya, Shakeel Ahmed, Esben Auken & Saurabh K. Verma (2019): Geological significance of delineating paleochannels with AEM, Exploration Geophysics, DOI: 10.1080/08123985.2019.1646098

To link to this article: https://doi.org/10.1080/08123985.2019.1646098

Published online: 25 Aug 2019.

EXPLORATION GEOPHYSICS
https://doi.org/10.1080/08123985.2019.1646098

Geological significance of delineating paleochannels with AEM

Subash Chandra[a], Joy Choudhury[a], Pradip K. Maurya[a,b], Shakeel Ahmed[a], Esben Auken[b] and Saurabh K. Verma[a]

[a]CSIR, National Geophysical Research Institute, Hyderabad, India; [b]HHG, Aarhus University, 8000 Aarhus C Denmark

ABSTRACT
Paleochannels typically act as pathways for groundwater movement and provide a potential source of groundwater. Their presence can be helpful in identifying areas suitable for recharge and at times in mitigating contamination problems in afflicted regions. Thus, mapping of paleochannels is significant in the planning and management of groundwater resources. An airborne electromagnetic (AEM) system employing dual pulse moments has been used extensively for this purpose in India. This paper presents the results over paleochannels defined in three different terranes. In northwest India, a 100 m wide by 80 m deep paleochannel within alluvium overlaying a Proterozoic basement illustrates the impact of neotectonic disturbances in changing the river course. In northeast India's Ganga Plains, a paleochannel is mapped that provides insight into managing groundwater resources of areas polluted with arsenic. In south India, a paleochannel buried under ∼ 100 m thick sequence of coastal sediments is imaged with implications on submarine groundwater discharge.

ARTICLE HISTORY
Received 1 October 2018
Accepted 11 July 2019

KEYWORDS
Airborne geophysics; aquifer; 3D modelling; hydrogeology; mapping; tectonics

Introduction

Shortage of fresh water is recognised as a major global issue, and India ranks high among the largest users of groundwater for irrigation (Suhag 2016). According to global groundwater extraction trends, India's water resources are depleting at an alarming rate, leading to severe scarcities in many parts of the country (Planning Commission 2007; Chandra et al. 2016a; Kant 2018). The composite water management index report of India reveals that the country is witnessing the most difficult water crisis in its history (Kant 2018). Around 600 million Indians face high to extreme water stress and 200,000 people die every year due to unsafe water consumption. The report further predicts that by 2030, the overall demand for water will be twice the currently available supply. In this gloomy situation, scientists, experts and policy-makers realise that a managed aquifer recharge (MAR) program could be one of the most effective and practical measures to control dwindling groundwater resources (Wright and Toit 1996; Bouwer 2002; Asano and Cotruvo 2004; Ong'or and Long-Cang 2009).

MAR requires knowledge of the structural settings of groundwater systems, spatial variability, connectivity, groundwater pathways, hydraulic property, etc. Thus mapping of the near surface with an emphasis on aquifers and paleochannels is important. To address this challenge, the Ministry of Water Resources, Government of India has launched a large program of aquifer mapping for effective management of groundwater resources (Ahmed et al. 2016; Chandra et al. 2016a, 2016b, 2017b; Chatterjee et al. 2018).

Paleochannels usually provide for potential resources of potable water. However, if contaminated, they can adversely affect large areas and deeper aquifers. Therefore, study of paleochannels is important in planning for MAR and devising strategies for contamination control and protection of fresh groundwater zones.

Paleochannels may be found exposed on the surface or buried, depending on the post-depositional environment. Buried paleochannels may have properties very similar to those of aquifers but are distinguished by their low width to length ratio. Also, whereas an aquifer is usually planar, a paleochannel can be tortuous in plan view. A variety of techniques have been used to map paleochannels; mostly ground-based geophysical techniques including gravity, seismic and electrical methods (e.g. Ghose, Kar, and Husain 1979; Fitterman et al. 1991; Sinha et al. 2006; Gupta, Sharma, and Sreenivasan 2011; Sinha et al. 2013; Francke 2016; Rastogi et al. 2016). Airborne geophysical surveys with their ability to rapidly cover large areas including inaccessible ones, are ideally suited to map paleochannels. However, there are few reports in the literature on using AEM to map paleochannels (Walker and Kroll 2010; Abraham et al. 2012). In this paper, we present AEM investigations that have successfully mapped paleochannels of varying dimensions in three different hydrogeological settings, viz.,

CONTACT Subash Chandra schandra75@gmail.com #119, Groundwater Building, CSIR-NGRI, Uppal Road, Hyderabad-500007 Telangana State, India

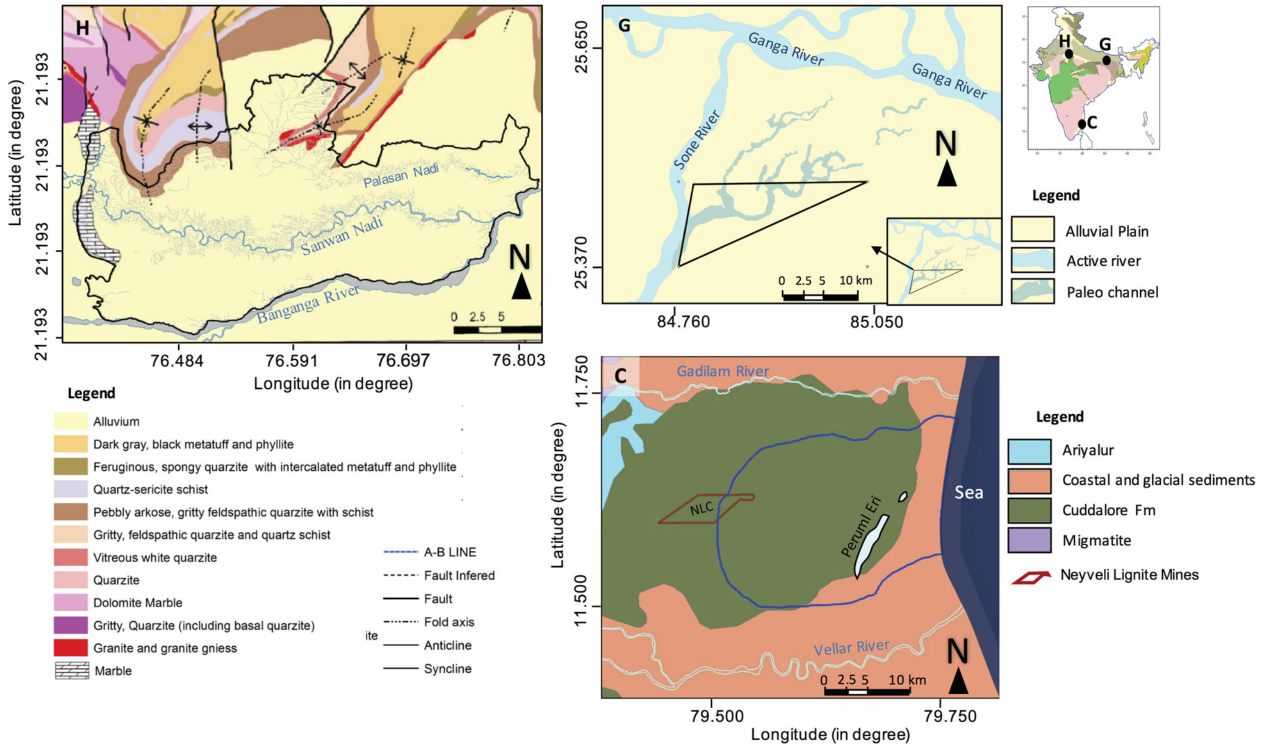

Figure 1. Location of the study areas, i.e. (H) hard rock terrain in Dausa district, Rajasthan, (G) alluvium in Ganga Plain, Patna district, Bihar and (C) coastal alluvium in Cuddalore district, Tamil Nadu, India.

alluvium-covered hard rock, Ganga River plains and coastal alluvium in India (Figure 1). The surveys were carried out employing dual moment SkyTEM304 and SkyTEM306 in 2013/14.

The study areas

Alluvium over hard basement, northwest India

The Dausa area in Rajasthan, northern India (hereafter termed as hard rock area) consists of Proterozoic quartzites, phyllites, limestones, schists and Archean gneisses that are found exposed on the Aravalli Hills along the northern boundary of the survey area. These rocks have undergone multiple episodes of folding and faulting (Naha et al. 1984; Naha, Mookherjee, and Sanyal 1987) and polyphase metamorphism. The area measuring 647 km^2 lies within latitude 26°56′36′′N and 27°10′36′′N and longitude 76°25′00′′E and 76°49′31′′E. After the main river Banganga, it is designated as "Banganga Watershed" that also includes a couple of seasonal tributaries flowing through the region. Banganga River forms the southern boundary of the area, whereas the northern boundary is covered by hills. There are two seasonal streams, Sanwan Nadi and Palasan Nadi, flowing almost parallel to the Banganga River and both finally join it at the eastern boundary of the area. Average annual rainfall in the study area is around 660 mm (Chatterjee et al. 2018). The major part of the area is covered by Quaternary alluvium. Groundwater overexploitation and high degree of salinity are the major issues in the region.

Ganga Plains, northeast India

The second study area forms part of the Sone Megafan in the Sone–Ganga alluvial tract located on the Ganga Plain in Bihar state, between latitudes 25°25′12′′N to 25°40′48′′N and longitudes 84°49′12′′E to 85°1′12′′E. The area receives an average normal monsoon rainfall of ∼ 1225 mm/year with large fluctuations in recent years (Sahu, Saha, and Shukla 2018). The Sone River flows from southwest to northeast and forms the western boundary of the survey area with a number of braided paleochannels (Sahu, Raju, and Saha 2010; Sahu and Saha 2014; Sahu, Saha, and Shukla 2018). The east-flowing Ganga River is located ∼ 20 km north of the survey area (Figure 1). Geologically, the area constitutes a thick sequence of Ganga alluvium resting on pre-Tertiary formations containing several aquifers. Both the Ganga and Sone rivers have moved over time, building up a sedimentary river basin with different types of sediments (i.e. clayey, silty, sandy) forming various types of aquifers due to the interactions of the two rivers. The area suffers from patchy arsenic contamination (Chandra et al. 2011).

Coastal alluvium, south India

The third example is from Cuddalore district in Tamil Nadu. Measuring 517 km^2, the coastal area in southern India forms a gentle slope characterised by Cuddalore formation and alluvium. Although outside, there are two eastward flowing rivers, i.e. Gadilam (in north) and Vellar (in south) that bound the study area. Flood plains are developed along the river courses with plains at the mouth. Sand bars are scattered along the course of the rivers. The coastal plain exhibits different geomorphic features that include beach ridges, dune complexes, mud flats, salt flats and salt pans. Cuddalore formation of Mio-Pliocene age comprises argillaceous sandstone, pebble-bearing sandstone, ferruginous sandstone, grits and clay beds. Sandstone of the Cuddalore series are whitish, pinkish, reddish or mottled in colour. Lignite deposits occur within these formations. Recent alluvium deposits comprise soils, blown sands, laterites and recent alluvium (Rameshkumar et al. 2014). The area suffers from groundwater salinity due to seawater intrusion and industrial wastes.

Survey specifications and methodology

The AEM survey was conducted using dual moment SkyTEM304 system in hard rock and SkyTEM306 in Ganga Plain and coastal alluvium with the objective to map the subsurface conductivity distribution down to maximum depths of 200 and 300 m, respectively. However, the presence of conducting overburden often results in reduced penetration depth. Both systems facilitate very early time measurements starting at $\sim$ 10 μs using the low moment and late time measurements up to $\sim$ 10 ms using high moment. In hard rock, the AEM data were acquired at 200 m flight line spacing. For Ganga Plain and coastal alluvium, the flight line spacing was 250 m. The data were acquired with the sensor height varying between 30 and 40 m above ground level at a flying speed between 60 and 80 km/h, which translates to a sample point at every 2.5–3 m along the flight line.

AEM data were processed using Aarhus Workbench following the standard processing scheme described by Auken et al. (2009). Soundings are created every 25–30 m by averaging the raw stacked data to improve the signal-to-noise (S/N) ratio. Data are then (1D) inverse-modelled using a laterally constrained inversion (LCI) scheme (Auken et al. 2005) and the ensuing results are used for quality checking and revisiting the data processing to ensure that noisy data are filtered out. Finally, the data were inverted employing spatially constrained inversion (Viezzoli et al. 2008) with smooth discretisation. Figure 2 further elucidates processing and modelling steps using data from Dausa area.

The derived resistivity model was validated with bore hole lithologs and geophysical logs, and then used to produce a 3D model comprising aquifer, paleochannels, aquitard or aquiclude, etc. The AEM mean resistivity map was analysed with depth to identify linear or curvilinear tracks with connectivity and continuity at regional (tens of kilometres) scale. Paleochannels are expected to show a contrast in resistivity: higher resistivities if carrying fresh water in, e.g. marine or clay-rich sediments, or lower values if containing salty water. However, to

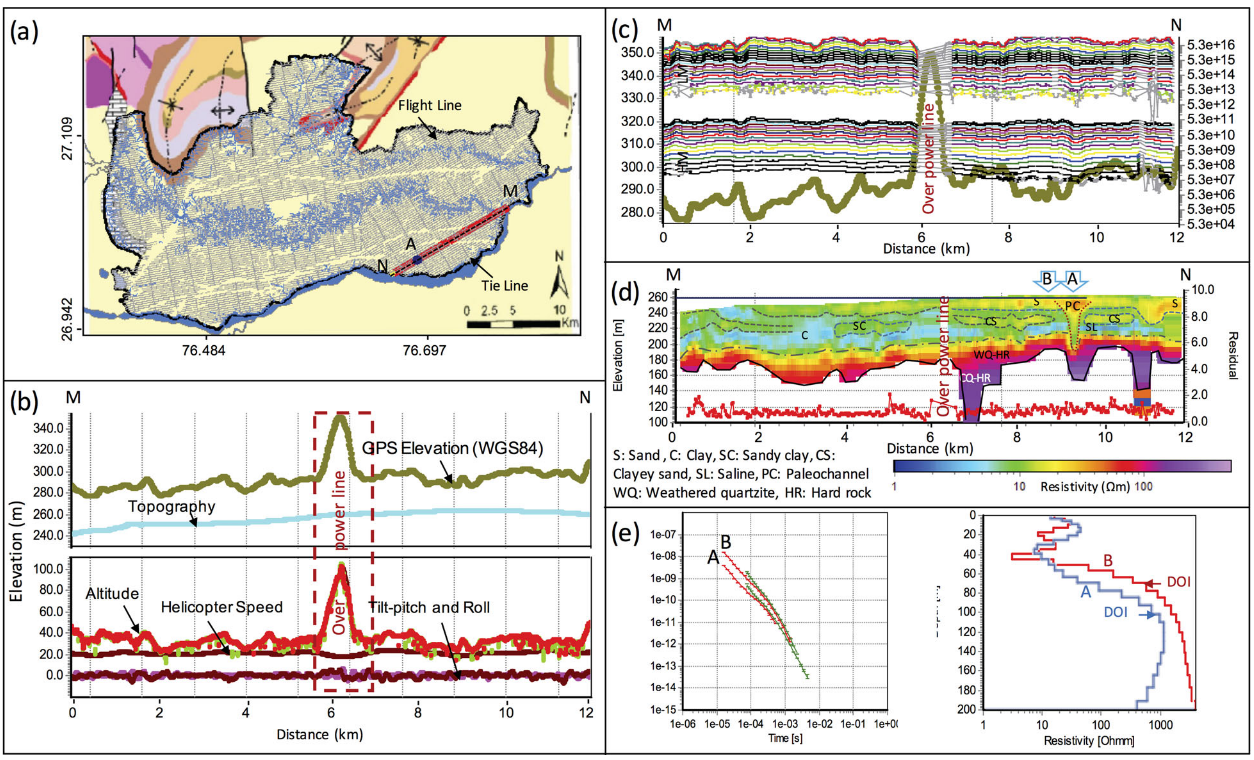

Figure 2. (a) Flight-line map after filtration over geological map, Dausa district, Rajasthan. (b) Parameter profile of 12 km flight showing height/elevation of the transmitter loop, ground topography (above mean sea level), altitude corrected (smoothed) line for ground clearance, helicopter speed, plus pitch and role. (c) Low and high moment average filtered data of corresponding 12 km flight lines between points M and N. (d) LCI resistivity image along the MN profile. (e) Acquired dB/dt response for low and high moment transmission at points A and B and their LCI 1D depth-resistivity smooth models.

identify a paleochannel, it is important to map a continuous linear/curvilinear feature with possible connectivity to some stream or water body.

Results and discussion

Paleochannel in hard rock terrain

AEM data were acquired along flight lines flown in two orientations, i.e. N60°E and N80°E, in respectively eastern and western parts of the area to cut across the major geological settings and power lines (Figure 2a). A 12 km profile (MN) is selected to show various processing parameters, namely: GPS elevation of the transmitter loop, the ground topography, pitch and roll, altitude corrections where reflections from the treetops are removed, average low and high moment data after decoupling, removal of late time noise, filtering (trapezoidal), and LCI-derived resistivity image (Figure 2). The data corresponding to high GPS elevation over power lines was filtered out (Figure 2c). Inverted resistivity model below the depth of investigation (DOI) (Christiansen and Auken 2012) line was removed. The ground surface is $\sim$ 240 m above mean sea level (amsl). In general, DOI is found at $\sim$ 160 m except for a few patches in the eastern half of the profile where it is deeper. The derived resistivity sections can be broadly divided into two main parts, i.e. an upper layer of alluvium with a relatively low resistivity in the range 1–50 Ωm, with an underlying hard rock layer with relatively high resistivity $\geq$ 50 Ωm (Figure 2d). The resistivity ranges can be classified as: 1–6 Ωm for a saline layer, 5–15 Ωm for a clay layer, 15–25 Ωm for silty or sandy clay, 20–35 Ωm for clayey sand, 35–100 Ωm for sand and 80–1000 Ωm or more for quartzite hard rock. The upper alluvium has two sandy layers of 15 m thickness separated by a 10 m thick clay-rich layer. AEM data have revealed an anomalous thick ($\sim$ 50 m) lens of resistive sand at point "A" (Figure 2d). This anomalous lens of resistive sand (PC in Figure 2d) turns into conductive depression at a deeper level (190–210 m elevation) in quartzite hard rock. TEM data at point A and B in its vicinity are compared in the form of dB/dt and smooth inverted depth-resistivity model (Figure 2e). Both dB/dt and inverted resistivity model depict noticeable contrasts at points A and B.

Depth slice resistivity maps at 5 m intervals were prepared from the ground surface down to 150 m. The variations in resistivities correlate strongly with the geology. For example, high-resistivity zones ($\sim$ 1000 Ωm) correspond to outcropping basement of quartzite, granite, limestone, etc., exposed over the western and northern boundaries as well as at depth within the survey area (Figure 3). The high-resistivity zone progresses eastwards with depth, suggesting an east-dipping bedrock. At point "A" a curvilinear (meandering) track, $\sim$ 100 m wide with $\sim$ 35 Ωm resistivity (sand), is noticeable within a conductive ($\sim$ 10 Ωm, clay) medium. It connects the Sanwan River at A_1 in the west and Banganga River at A_2 in the east. This consistent resistive feature gets thinner and more prominent with depth, as seen in the mean resistivity maps at 20–25 m (Figure 3b), 30–35 m (Figure 3c) depths, and extends down to 50 m depth in alluvium. However, the resistive curvilinear feature appears as a conductive track in the underlying quartzite background (see mean resistivity map of 60–65 m in Figure 3d). The conductive feature slowly disappears at around 85 m depth. This anomalous track is interpreted as a paleochannel of Sanwan Nadi. The upper (50 m) high-resistivity zone of the paleochannel suggests coarse, permeable sediments deposited where the paleochannel has cut through clay-rich alluvium. The quartzite bedrock is encountered at $\sim$ 50 m depth and the paleochannel here exhibits as a zone of low resistivity relative to the quartzite host medium. The resistivity cross section along 1.5 km long profiles L_1L_1' and L_2L_2' derived from the interpolated 3D resistivity grid clearly shows the paleochannel as a resistive anomaly revealing coarse-grain deposits (Figure 3e and 3f). The resistivity profiles in general show a low-resistivity ($\sim$ 10 Ωm) layer at 230 m elevation running almost horizontal. The change in the river's course is interpreted as being due to tectonic disturbances; a conclusion supported by the presence of number of closely spaced folds and faults in the area.

The inferred paleochannel is $\sim$ 100 m wide at 60 m depth. A 3D model of the subsurface showing the paleochannel and the current position of Sanwan Nadi is shown in Figure 4. The delineation of the $\sim$ 100 m wide zone at around 50–80 m depth illustrates the capability of the AEM system for high-resolution mapping. The AEM dense data acquisition with a high S/N ratio and an advance level of processing and inversion has resulted in a much better result compared with that obtained by ground surveys.

Paleochannel in Ganga Plains

The Sone River originates near Amarkantak in Madhya Pradesh, central India and joins river Ganga near Patna as its second largest tributary. The Sone River is notorious for changing its course due to a steep gradient and high flow rates. In the ancient past, the Sone flowed east of the current position, which implies that the confluence of the Sone and Ganga rivers has been shifting westwards. The AEM survey covers part of a paleochannel that can be seen in the resulting resistivity images (Figure 5). The area is affected by arsenic contamination, which is of increasing concern due to its high toxicity and rapid spread in the Middle and Upper Ganga Plain. It is worth mentioning that the problem of arsenic contamination is severe in Bangladesh (Chandra et al. 2011), and this work suggests a regional westward extension of the contamination in the upstream region

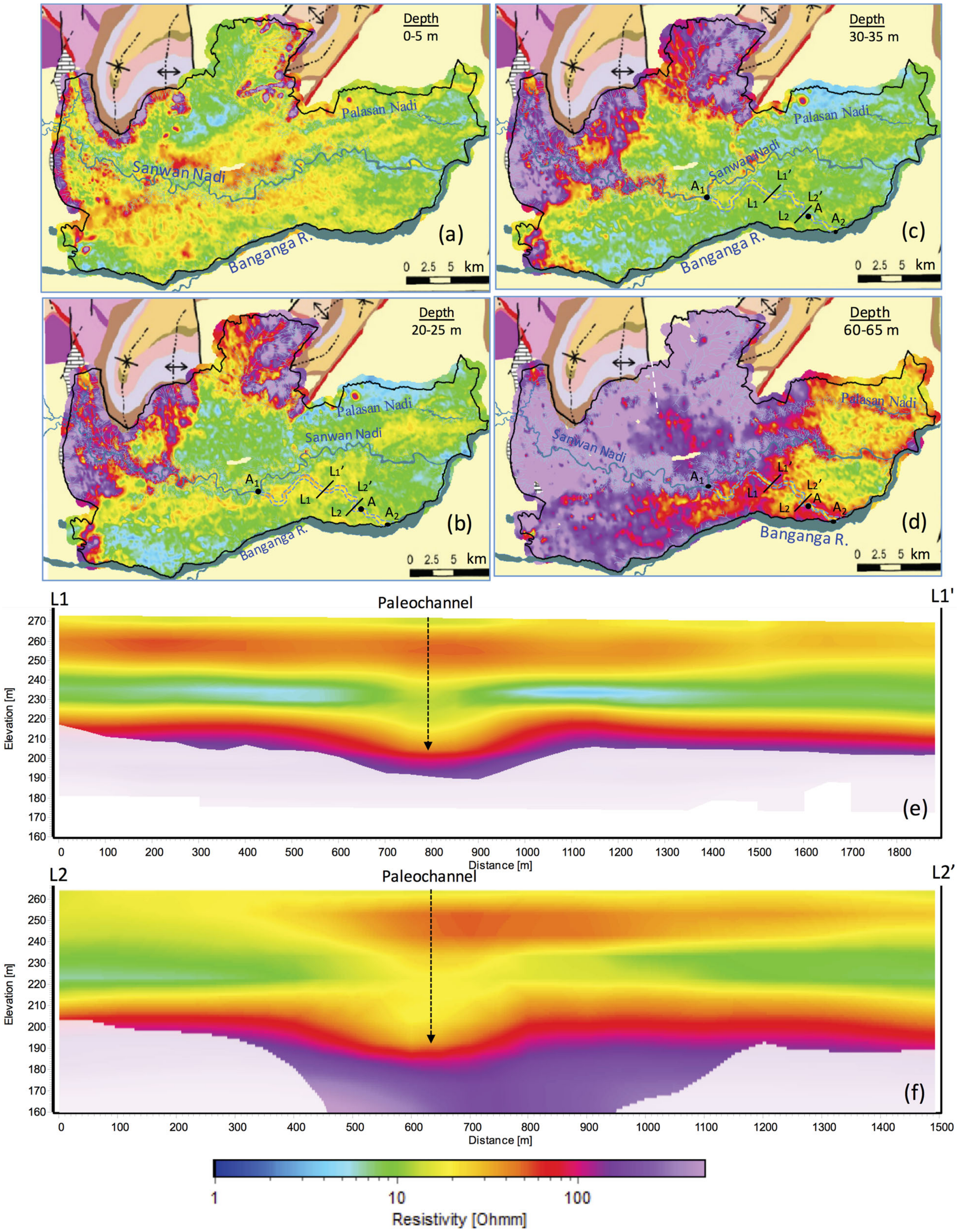

Figure 3. Resistivity depth slices of alluvium covered hard rock terrain, Rajasthan for depths: (a) 0–5 m, (b) 20–25 m, (c) 30–35 m and (d) 60–65 m showing track of the inferred paleochannel. (e,f) Resistivity cross section derived from the interpolated 3D resistivity grid along profiles (e) L_1L_1' and (f) L_2L_2' traversing the paleochannel.

(Chakraborti et al. 2003). Previous studies (Acharya 2005; Kumar et al. 2010) indicate that, apart from geochemical factors responsible for the arsenic contamination in Ganga Plains, mechanical factors may also be responsible for the spread of contamination downwards and laterally. Initially only shallow aquifer, Aq-1, was contaminated, which led to exploitation of a deeper ($\sim$ 100 m) aquifer, Aq-2 (Figure 5). Differential pumping (a little from Aq-1 and a lot from Aq-2) led to vertical percolation of arsenic contamination to the

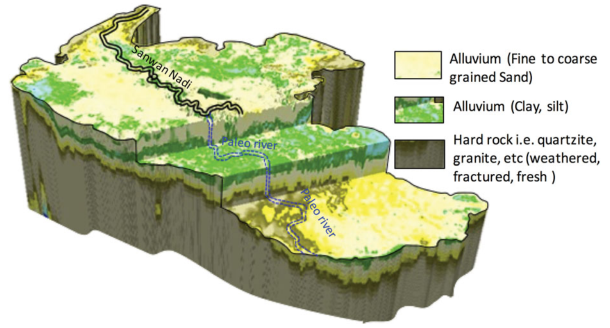

Figure 4. 3D lithological model of alluvium-covered hard rock terrain, Rajasthan showing the current path of Sanwan Nadi and its interpreted paleo path.

deeper aquifer (Muralidharan 1998; Mukherjee, Fryar, and Howell 2007). The studies show that older sediments in the Ganga Plains in parts of Uttar Pradesh and Bihar are free from arsenic contamination, whereas the organic-rich grey to black younger (Holocene) alluvium are rich in arsenic (Acharya and Shah 2007; Shah 2008; Shah 2017). It is also observed that most of the arsenic-affected areas in the Ganga Plains are preferentially located close to the abandoned channel or the present river. Differential pumping is likely to lead to a spread of contamination from younger alluvium to older alluvium mechanically if they are not separated by an impermeable (e.g. clay) layer. Thus, knowledge of the stratigraphy may be insufficient for effective planning of groundwater management. Some knowledge of aquifer systems and impermeable (clay/silt) layer distribution in 3D at a regional scale is also needed before devising an effective groundwater management plan to control the spread of arsenic contamination.

In spite of a large number of studies on geochemical aspects and design of various filters (Shen 1973; Hering et al. 1997; Ning 2002; Bissen and Frimmel 2003; Cheng et al. 2004; Shih 2005; Dodd et al. 2006; Feistel et al. 2016; Otter et al. 2017), it has been found that local attempts to supply arsenic-free water suffer from many problems including lack of a proper waste disposal system, irregular or no power supply and poor maintenance (Ghosh and Singh 2010; Chandra et al. 2011). Hence, they do not provide a sustainable solution. Studies by Chandra et al. (2011) in the Ganga Plain have found that the clay acts as a barrier to the spread of arsenic contamination. Thus, hydrodynamic balance

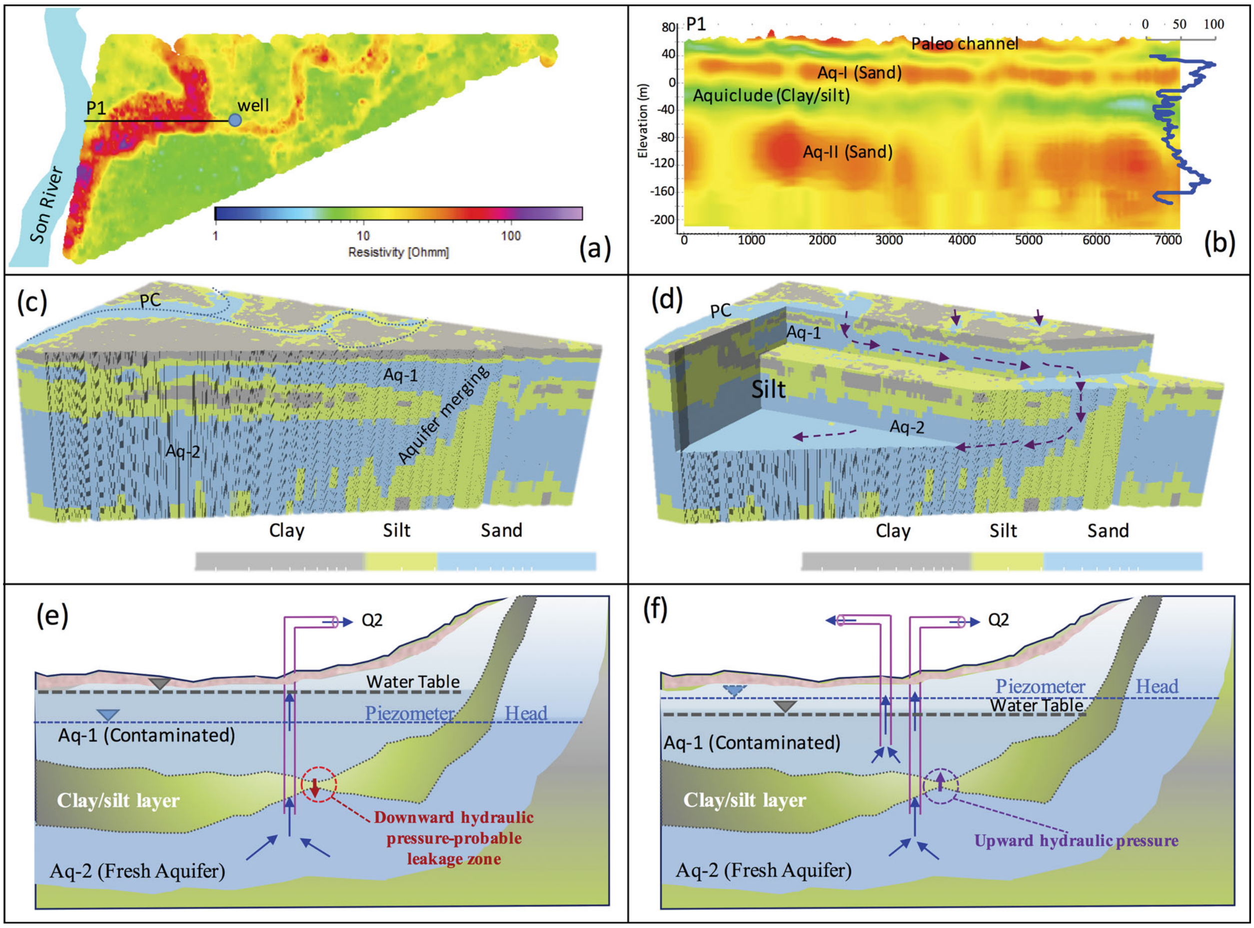

Figure 5. (a) Resistivity depth slice for map at depth 0–10 m for Ganga alluvium, (b) interpreted resistivity profile, (c) 3D aquifer model showing paleochannel, principal aquifers 1 and 2, and zone of aquifer merging. (d) 3D aquifer cutaway model showing connectivity between paleochannel and Aq-1 and Aq-2. (e) Schematic model showing downward hydraulic pressure inducing leakage from Aq-1 to Aq-2 due to heavy pumping from the deeper aquifer. (f) Twin pumping from shallow and deeper aquifer in such a way that piezometers remain above the water table to avoid contamination (of arsenic) to the deeper aquifer.

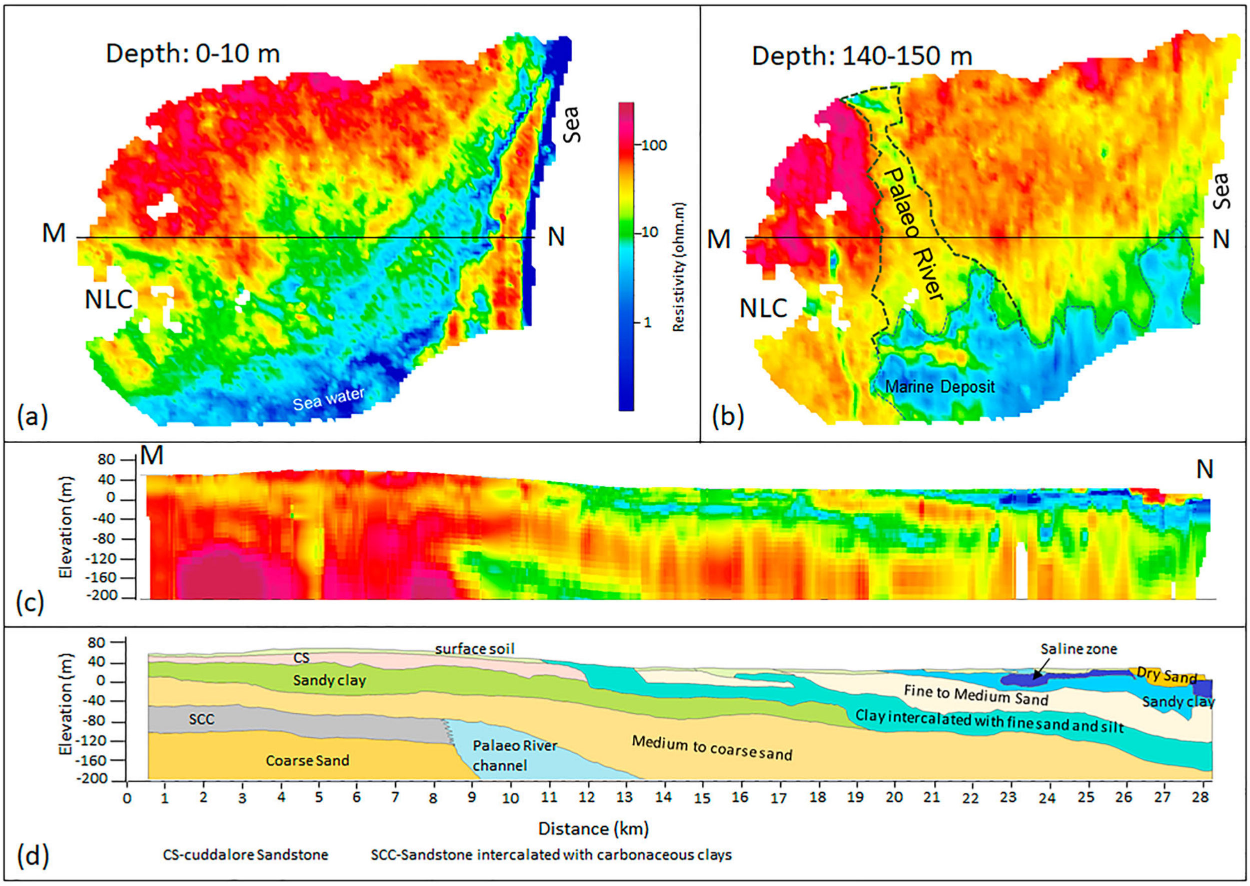

Figure 6. Resistivity depth slice for coastal plain at depth (a) 0–10 m and (b) 140–150 m with inferred paleochannel and marine deposits. (c) Resistivity profile along PQ and (d) interpreted lithological model with inferred buried paleochannel

combined with a good knowledge of the hydrogeological framework may yield a sustainable solution for managing safe aquifer exploitation in arsenic-affected regions in the survey area.

The AEM survey results revealed high resistivity over the paleochannel due to its freshwater content in medium to coarse sand (Figure 5a). The paleochannel is found to vary in width from a few hundred of metres to a few kilometres with a maximum depth extending down to $\sim$ 30 m. The resistivity section in Figure 5(b) shows the location of the paleochannel along with the first and second principal aquifers, with mapped thicknesses of 40 and 140 m, respectively. The AEM results reveal that the paleochannel is connected to the first principal aquifer, which in turn merges with the second deeper aquifer along an interpreted fault plane (Figure 5c and 5d). Interpreted pathways depicting the interconnectivity of permeable zones are shown in Figure 5(d). Knowledge of the paleochannel and its connectivity to the aquifer systems can be used to manage aquifer recharge as well as mitigate groundwater contamination. It is important to manage the hydraulic balance between the water table of the first upper aquifer and the piezometric level of the second lower aquifer. Pumping only from the second aquifer, as happened with most of the wells in Bangladesh, may result in lowering of the piezometric level below the water table, resulting in downward hydraulic pressure. In such conditions, leaky layers may allow vertical percolation of arsenic contamination (Figure 5e). If dual pumping is carried out, i.e. pumping from both aquifers, in such a way that the piezometric level remains above the water table and upward hydraulic pressure is maintained, then downward percolation of arsenic contamination can be avoided (Figure 5f). The 3D aquifer geometry required before optimal pumping can occur is best obtained from an AEM survey.

Buried paleochannel in coastal alluvium

The third example is from the coastal area in Cuddalore district of Tamil Nadu. The top (0–10 m) mean resistivity depth slice shows a resistive ($\geq$ 50 Ωm) area in the northwest with a similar north–south strip on the eastern side and low resistivities, down to $\leq$ 1 Ωm in between with decreasing values towards the south (Figure 6a). The high resistivities in the northwest indicate that the upper 10 m layer, including surface soil, is composed of medium- to coarse-grained sediments, favourable for high infiltration and percolation and hence a suitable site for MAR. The AEM resistivity is $\leq$ 1 Ωm over seawater at the coast. Thus, zones with $\sim$ 1 Ωm resistivity are interpreted as seawater at the coast, or seawater intrusion if located away from coast.

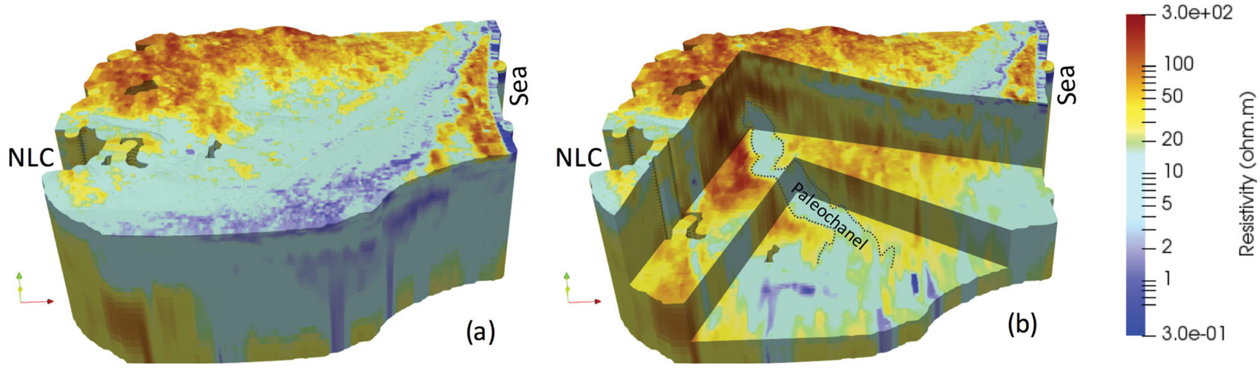

Figure 7. (a) 3D resistivity model for coastal plain. (b) Cutaway 3D resistivity model showing buried paleochannel.

The resistivity map (0–10 m depth, Figure 6a) shows connectivity between the southern part of the survey and the coast at the northeast margin through conductive ($< 1\ \Omega$m) pathways indicating seawater intrusion. The southern zone is found to be conductive ($\sim 3\ \Omega$m) down to 150 m depth, which is inferred as marine sediments.

The AEM results reveal an almost horizontal stratigraphy from the western boundary for $\sim$ 8 km eastwards towards the coast (profile MN) and thereafter the strata dips towards the coast (Figure 6c and 6d) displaying a natural depositional environment. However, at deeper levels, a conductive linear feature is encountered at $\sim$ 80–120 m that extends to 250 m depth. This is interpreted as a buried paleochannel. Figure 7 shows the 3D resistivity model in full plus a cutaway view highlighting the paleochannel. The paleochannel exhibits relatively low resistivity due to mixing of saline and fresh waters. The channel trends southeasterly towards the coast, getting wider with depth, implying that the paleochannel originally flowed from northwest to southeast, moving westward over time. A thick sedimentary overburden suggests a high rate of sediment deposition that coupled with neo-tectonic activity probably caused a narrowing of the river until it closed off. The shallowing of the paleochannel towards the northwest suggests that this paleochannel may have been an earlier course of the Gadilam River which currently flows from west to east along the northern boundary of the study area (Figure 1).

Conclusions

Results from three large, different hydrogeological settings (i.e. hard rock, Ganga Plains and coastal alluvium) clearly demonstrate that AEM surveys can be very effective for mapping paleochannels. The paleochannel mapped in the hard rock region would have been difficult if not impossible to map using a ground survey. Establishing linearity and continuity of such a thin channel with a negligible surface signature is difficult unless mapping is done on a regional scale. The paleochannel in the Ganga Plain is an easy target as it has a visible surface signature; however, its characterisation and connectivity with the aquifer system are important in designing a better management plan to protect the deeper fresh aquifer from arsenic contamination. The 3D structure of the buried paleochannel in the coastal plain in South India reveals that the river was flowing southeast and migrated away from the coast over time in a depositional environment. The width of the paleochannel reduced as it was getting shallower due to sediment deposition and migration.

The results demonstrate that with dense data sampling and sensitivity to small changes in conductivity, AEM is efficacious in mapping subsurface features like paleochannels. The regional coverage is found to be particularly useful in establishing their continuity and connectivity.

Acknowledgments

This work forms part of the Aquifer Mapping pilot project funded by the Central Ground Water Board, Ministry of Water Resources, River Development and Ganga Rejuvenation, GOI. We thank the Director, CSIR-NGRI for the necessary approval and support. The entire AQUIM team and those who have directly or indirectly contributed to the project in conceptualisation, discussions and execution are also duly acknowledged. We gratefully acknowledge the constructive and critical comments/suggestions by Dr Andreas A. Pfaffhuber, Associate Editor and the reviewers (Dr John Bishop and Dr Jared Abraham) that significantly improved the quality of the paper.

Disclosure statement

No potential conflict of interest was reported by the authors.

Funding

This work is supported by Ministry of Jal Shakti, Department of Water Resources, River Development & Ganga Rejuvenation (http://mowr.gov.in/) [grant number SSP-659-28(SA)].

References

Abraham, J.D., J.C. Cannia, P.A. Bedrosian, M.R. Johnson, L.B. Ball, and S.S. Sibray. 2012. Airborne electromagnetic mapping of the base of aquifer in areas of western Nebraska: *U.S. Geological Survey Scientific Investigations Report*2011–5219: 38.

Acharya, S.K. 2005. Arsenic levels in groundwater from quaternary alluvium in the Ganga Plain and the Bengal basin, Indian subcontinent: Insights into influence of stratigraphy. *Godwin Research* 8, no. 1: 55–66.

Acharya, S.K., and B.A. Shah. 2007. Groundwater arsenic contamination affecting different geologic domains in India – a review: Influence of geological setting, fluvial geomorphology and quaternary stratigraphy. *Journal of Environmental Science and Health A* 42: 1795–1805.

Ahmed, S., S. Chandra, S.K. Varma, D. Muralidharan, R. Rangarajan, N.C. Mondal, S. Sonkamble, E. Nagaiah, V.K. Somvanshi, and D.V. Reddy. 2016. Synoptic report: pilot aquifer mapping (AQUIM) project - Findings, Efficacy & Protocols. *NGRI Tech Report* No. NGRI-2016-GW-900.

Asano, T., and J.A. Cotruvo. 2004. Groundwater recharge with reclaimed municipal wastewater: Health and regulatory considerations. *Water Research* 38: 1941–1951.

Auken, E., A.V. Christensen, B.H. Jacobson, N. Foged, and K.I. Sorensen. 2005. Piecewise 1D laterally constrained inversion of resistivity data. *Geophysical Prospecting* 53: 497–506.

Auken, E., A.V. Christensen, J.H. Westergaard, C. Kirkegaard, N. Foged, and A. Viezzoli. 2009. An integrated processing scheme for high-resolution airborne electromagnetic surveys, the SkyTEM system. *Exploration Geophysics* 40: 184–192.

Bissen, M., and F.H. Frimmel. 2003. Arsenic—A review. Part II: Oxidation of arsenic and its removal in water treatment. *Acta Hydrochimica Hydrobiologica* 31: 97–107.

Bouwer, H. 2002. Artificial recharge of groundwater: hydrogeology and engineering. *Hydrogeology Journal* 10: 121–142.

Chakraborti, D., S.C. Mukherjee, S. Pati, M.K. Sengupta, M.M. Rahman, U.K. Chowdary, D. Lodh, C.R. Chanda, A.K. Chakraborti, and G.K. Basu. 2003. Arsenic groundwater contamination in middle Ganga Plain, Bihar, India: A future danger? *Environmental Health Perspectives* 111: 1194–1201.

Chandra, S., S. Ahmed, E. Auken, J.B. Pedersen, A. Singh, and S.K. Varma. 2016a. 3D aquifer mapping employing airborne geophysics to meet India's water future. *The Leading Edge* 35, no. 9: 770–774.

Chandra, S., S. Ahmed, E. Nagaiah, S.K. Singh, and P.C. Chandra. 2011. Geophysical exploration for lithological control of arsenic contamination in groundwater in middle Ganga Plains, India. *Physics and Chemistry of the Earth* 36: 1353–1362.

Chandra, S., E. Nagaiah, N. Veerababu, N.C. Mondal, V.K. Somvanshi, and S. Ahmed. 2016b. Advanced geophysical investigation including Heliborne TEM in high-resolution aquifer mapping with special emphasis on crystalline hard rocks. *Special publication* in *Journal of Geological Society of India* 5: 87–96.

Chatterjee, R., A.K. Jain, S. Chandra, V. Tomar, P.K. Parchure, and S. Ahmed. 2018. Aquifer mapping and management in water stressed Baswa-Bandikui watershed, Dausa district, Rajasthan, India. *Environmental Earth Science* 77: 157.

Cheng, Z., A. van Geen, C. Jing, X. Meng, A. Seddique, and K.M. Ahmed. 2004. Performance of a household-level arsenic removal system during 4-Month deployments in Bangladesh. *Environmental Science and Technology* 38: 3442–3448.

Christiansen, A.V., and E. Auken. 2012. A global measure of depth of investigation. *Geophysics* 77, no. 4, WB171-WB171,6 FIGS.

Dodd, M.C., N.D. Vu, A. Ammann, C. Van Le, R. Kissner, H.V. Pham, T.H. Cao, M. Berg, and G.U. Gunten. 2006. Kinetics and mechanistic aspects of As(III) Oxidation by Aqueous Chlorine, Chloramines, and Ozone: Relevance to drinking water treatment. *Environmental Science and Technology* 40: 3285–3292.

Feistel, U., P. Otter, S. Kunz, T. Grischek, and J. Feller. 2016. Field tests of a small pilot plant for the removal of arsenic in groundwater using coagulation and filtering. *Journal of Water Process Engineering* 14: 77–85.

Fitterman, D.V., M.M. Christopher, M.A. Kamali, and F.E. Jama. 1991. Electromagnetic mapping of buried paleochannels in eastern Abu Dhabi Emirate, UAE. *Geoexploration* 27: 111–133.

Francke, J. 2016. *Mapping paleochannels in the Livbyan Sahara with ground penetrating radar*. 16th International conference on Ground Penetrating Radar (GPR), 1–5.

Ghose, B., A. Kar, and Z. Husain. 1979. Lost courses of the Saraswati river in the great Indian desert: New evidence from landsat imagery. *Geographical Journal* 145, no. 3: 446–451.

Ghosh, N.C., and R.D. Singh. 2010. Groundwater Arsenic contamination in India: Vulnerability and scope for remedy. https://www.semanticscholar.org/paper/Groundwater-Arsenic-Contamination-in-India-%3A-and-Ghosh-Singh/971302567d3b38e676f27dd69ec1af05bf06bfd8.

Gupta, A.K., J.R. Sharma, and G. Sreenivasan. 2011. Using satellite imagery to reveal the course of an extinct river below the Thar desert in the Indo-Pak region. *International Journal of Remote Sensing* 32: 5197–5216.

Hering, J.G., P.-Y. Chen, J.A. Wilkie, and M. Elimelech. 1997. Arsenic removal from drinking water during coagulation. *Journal of Environmental Engineering* 123: 800–807.

Kant, A. 2018. Composite water management index- a tool for water management, *NITI Ayog report*, 180.

Kumar, P., M. Kumar, A.L. Ramnathan, and M. Tsujimura. 2010. Tracing the factors responsible for arsenic enrichment in groundwater of the middle Gangetic Plain, India: a source identification perspective. *Environmental Geochemistry and Health* 32: 129–146.

Mukherjee, A., A.E. Fryar, and P.D. Howell. 2007. Regional hydro stratigraphy and groundwater flow modeling in the arsenic-affected areas of the western Bengal basin, West Bengal, India. *Hydrogeology Journal* 15: 1397–1418.

Muralidharan, D. 1998. Protection of deep aquifers from arsenic contamination in Bengal Basin. *Current Science* 75, no. 4: 351–353.

Naha, K., A. Mookherjee, and B.K. Sanyal. 1987. Deformation structures in the Rajpura-Darbia area, Rajasthan, Western India and their significance. In *Crustal evolution and orogeny*, ed. S.P.H. Sychanthavong, 275–291. New Delhi: Oxford and IBH Publ. Co.

Naha, K., D.K. Mukhopadhyay, R. Mohanty, S.K. Mitra, and T.K. Biswal. 1984. Significance of contrast in the early stages of the structural history of the Delhi and the pre-Delhi rock groups in the Proterozoic of Rajasthan, western India. *Tectonophysics* 105: 193–206.

Ning, R.Y. 2002. Arsenic removal by reverse osmosis. *Desalination* 143: 237–241.

Ong'or, B.T.I., and S. Long-Cang. 2009. Groundwater overdraft and the impact of artificial recharge on groundwater quality in a cone of depression, Jining, China. *Water International* 34, no. 4: 468–483.

Otter, P., P. Malakar, B.B. Jana, T. Grischek, F. Benz, A. Goldmaier, U. Feistel, J. Jana, S. Lahiri, and J.A. Alvarez. 2017. Arsenic removal from groundwater by Solar driven Inline-electrolytic induced Co-precipitation and filtration—a long term field test conducted in west Bengal. *International Journal of Environmental Research and Public Health* 14, no. 10: E1167.

Planning commission. 2007. Report of the expert Group on ground water management and ownership. http://planningcommission.nic.in/reports/genrep/rep_grndwat.pdf.

Rameshkumar, N., D. Gnansundar, B. Gowtham, and M. Senthilkumar. 2014. Disposition of aquifer system in parts of Gadilam, Paravanar, lower Vellar Watershed, Cuddalore district, Tamil Nadu. *International Journal Of Geomatics and Geosciences* 5, no. 2: 266–274.

Rastogi, B.K., G.C. Kothyari, B. Sairam, G.P. Kumar, V. Patel, O.P. Goswami, and N. Prajapati. 2016. Geophysical evidences for palaeochannels and possible sources of groundwater: A case study from kachchh region, western peninsular India. *Journal of Earthquake Science and Engineering* 3: 1–17.

Sahu, S., N.J. Raju, and D. Saha. 2010. Active tectonics and geomorphology in the Sone–Ganga alluvial tract in mid-Ganga basin, India. *Quaternary International* 227, no. 2: 116–126.

Sahu, S., and D. Saha. 2014. Geomorphologic, stratigraphic and sedimentologic evidences of tectonic activity in Sone–Ganga alluvial tract in Middle Ganga Plain, India. *Journal of Earth System Sciences* 123, no. 6: 1335–1347.

Sahu, S., D. Saha, and S.R. Shukla. 2018. Sone megafan: A non-Himalayan megafan of craton origin, forming a potential groundwater reservoir in marginal parts of Ganga Basin, India. *Hydrogeology Journal* 26, no. 8: 2891–2917.

Shah, B.A. 2008. Role of Quaternary stratigraphy on arsenic contaminated groundwater from parts of Middle Ganga Plain, UP-Bihar, India. *Environmental Geology* 53: 1553–1561.

Shah, B.A. 2017. Groundwater arsenic contamination from parts of the Ghaghara Basin, India: Influence of fluvial geomorphology and Quaternary morphostratigraphy. *Applied Water Science* 7, no. 5: 2587–2595.

Shen, Y.S. 1973. Study of arsenic removal from drinking water. *Journal - American Water Works Association* 65, no. 8: 543–548.

Shih, M. 2005. An overview of arsenic removal by pressure driven membrane process. *Desalination* 172: 85–97.

Sinha, R., K. Gaurav, S. Chandra, and S.K. Tandon. 2013. Exploring the channel connectivity structure of the August 2008 avulsion belt of the Kosi River, India- Application to flood risk assessment. *Geology* 41, no. 10: 1099–1102.

Sinha, R., S.K. Tandon, P. Sanyal, M.R. Gibling, D. Stuben, Z. Berner, and P. Ghazanfari. 2006. Calcretes from a late Quaternary interfluve in the Ganga plains, India: Carbonate types and isotopic systems in a monsoonal setting. *Palaeogeography, Palaeoclimatology, Palaeoecology* 242: 214–239.

Suhag, R. 2016. Overview of groundwater in India, *PRS Legislative Research report*, 11.

Viezzoli, A., A.V. Christiansen, E. Auken, and K.I. Sørensen. 2008. Quasi-3D modeling of airborne TEM data by spatially constrained inversion. *Geophysics* 73: F105–F113.

Walker, S.E., and A. Kroll. 2010. Airborne electromagnetic signature of a paleochannel uranium deposit: *ASEG 2010 - Sydney, Australia*, *1–3*.

Wright, A., and I.d. Toit. 1996. Artificial recharge of urban wastewater, the key component in the development of an industrial town on the arid west coast of South Africa. *Hydrogeology Journal* 4: 118–129.